Projection Optics for Extreme Ultraviolet Lithography (EUVL) Micro-field Exposure Tools (METs) with a Numerical Aperture of 0.5

Holger Glatzel*[1], Dominic Ashworth[2], Mark Bremer[1], Rodney Chin[1], Kevin Cummings[2], Luc Girard[1], Michael Goldstein[2], Eric Gullikson[3], Russ Hudyma[4], Jim Kennon[1], Bob Kestner[1], Lou Marchetti[1], Patrick Naulleau[3], Regina Soufli[5], Eberhard Spiller[6]

[1]Zygo Corporation, Extreme Precision Optics (EPO), Richmond, CA 94806, USA
[2]SEMATECH, Albany, NY 12203, USA
[3]Center for X-Ray Optics, Lawrence Berkeley National Laboratory, Berkeley, CA 94720, USA
[4]Hyperion Development, San Ramon, CA 94582, USA
[5]Lawrence Livermore National Laboratory, Livermore, CA 94550, USA
[6]Spiller X-ray Optics, Livermore, CA 94550, USA

ABSTRACT

In support of the Extreme Ultraviolet Lithography (EUVL) roadmap, a SEMATECH†/CNSE‡ joint program is under way to develop 13.5 nm R&D photolithography tools with small fields (micro-field exposure tools [METs]) and numerical apertures (NAs) of 0.5. The transmitted wavefront error of the two-mirror optical projection module (projection optics box [POB]) is specified to less than 1 nm root mean square (RMS) over its 30 μm × 200 μm image field. Not accounting for scatter and flare losses, its Strehl ratio computes to 82%. Previously reported lithography modeling on this system [1] predicted a resolution of 11 nm with a k-factor of 0.41 and a resolution of 8 nm with extreme dipole illumination. The POB's magnification (5X), track length, and mechanical interfaces match the currently installed 0.3 NA POBs [2] [3] [6], so that significant changes to the current tool platforms and other adjacent modules will not be necessary. The distance between the reticle stage and the secondary mirror had to be significantly increased to make space available for the upgraded 0.5 NA illumination modules [1].

This manuscript discusses the on-going efforts to develop and fabricate this optical projection module.

Keywords: EUV, lithography, aberrations, projection optics, multilayer coatings, wavefront metrology, optics fabrication.

1. INTRODUCTION

Over the history of semiconductor-based computing hardware, the microchip performance doubled approximately every two years ("Moore's law") [4]. Large consortiums have been pivotal towards procuring the resources for tackling the associated technical and financial challenges. SEMATECH has been enabling resist materials research through access to micro exposure tools (MET) for 157 nm, 193 nm immersion, and extreme ultraviolet lithography (EUVL) [16] [17] [18]. Over the past 7 years the current two SEMATECH 0.3 NA EUV METs have been supporting EUV resist materials readiness for a 22/16 nm half-pitch EUV introduction [3] [14] [15]. However, a higher NA next generation EUV MET is needed to support materials development for 11 nm half-pitch and smaller features sizes. SEMATECH completed the design of such a 0.5 NA MET in 2007 [1] and started the build of the system in late 2011 with the goal to have two such systems available for supporting materials research in early 2014. The optical design of its projection optics modules is based on a modified Schwarzschild design. The key distinction to a Schwarzschild optic is that its mirrors are 16th order aspheres with separated centers of curvature while a Schwarzschild optic uses two concentric spheres.

To upgrade the 0.3 NA METs, a 0.5 NA system (MET5) was designed and proposed with an 11 nm target resolution goal [1]. The primary purpose of these small field (20 μm × 300 μm) tools is to provide very early learning into the extendibility of EUV lithography and in particular in the areas of resists and mask architecture and to help drive materials / technology learning in both areas for patterning at 11 nm half-pitch and below. Given that 0.33 NA high-volume manufacturing (HVM) tools, in principle, capable of 16 nm resolution are now being deployed, it is crucial that advanced learning platforms such as the MET5 be capable of significantly higher resolution.

The Extreme Precision Optics (EPO) group of Zygo Corporation was chosen to lead the challenging development effort to upgrade the optical projection module of the MET3. This effort requires the merging of EUV-quality aspheric optics fabrication, EUV state-of-the-art multi-layer coatings, precision mechanical assembly and alignment and precision electro-mechanical control.

This manuscript outlines the on-going activities to develop and fabricate these modules.

The following topics will be discussed: design constraints and requirements, fabrication and metrology of the mirror substrates, multilayer coatings, opto-mechanical design, module assembly and metrology of the transmitted wave front. Furthermore, first lithographic modeling results will be presented.

2. DESIGN CONSTRAINTS AND REQUIREMENTS

The design for the MET5 originally came out of the realization that existing 0.3 NA (MET3) tools would eventually reach the limit of patterning resolution [1]. This is a natural progression and the MET3 itself was conceived when the earlier small field, 0.1 NA 10X Schwarzschild systems in use began to reach the end of their useful lives [5]. The main difference this time is that in addition to having sub-16 nm patterning expectations, the MET5 design would also have to be compatible with the existing MET3 platforms [6].

The 0.5 NA design of the MET5 gave us a comfortable 0.59 Rayleigh criterion at 16 nm resolution, however the need to re-use the MET3 platform imposed some difficult design constraints.

Figure 1 shows the high quality aerial image which can be expected from the MET5 for a simply scaled 16 nm planar 6T-SRAM bit cell gate array without proximity correction. Unbiased pattern formation happens at a 54% threshold with a normalized image log slope of 2 and image contrast of 72%. This led us to consider an 11 nm target resolution for the SEMATECH Albany platform, and an even better resolution for the flexible illumination available at LBNL where a new platform is being constructed. More detailed performance modeling is shown later in this paper. The Albany platform interface requirements determined track length, back working distance, maximum secondary diameter, mass and center of mass location. Other design choices were based on tradeoffs found through simulation. Table 1 shows the resulting MET5 key design requirements.

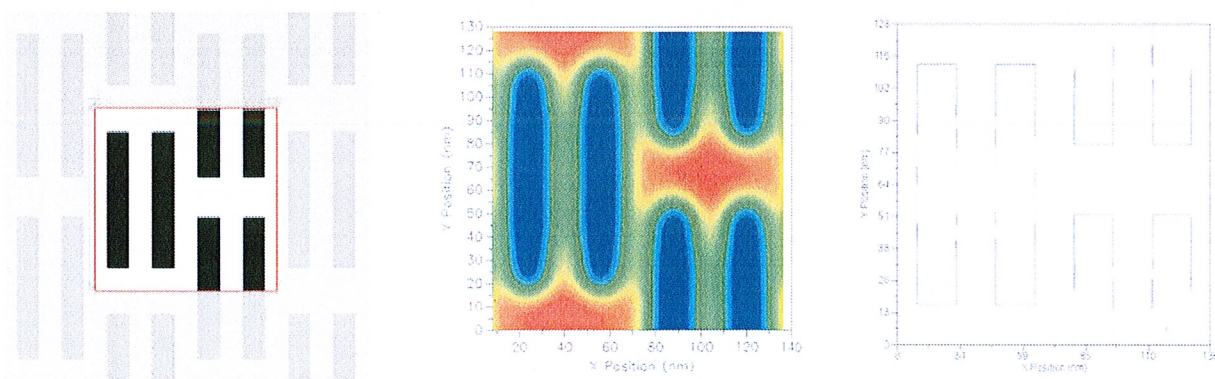

(a) Bit Cell Layout **(b) Aerial Image** **(c) Overlay of the Mask and Aerial Image Contours**

Figure 1. Rigorous electromagnetic thick-mask model of a simply scaled 16 nm SRAM gate array. Model parameters were: a chief ray angle of 6°, 0.35/0.70 annular illumination, 0.5 NA, 10% central obscuration by area, 5% flare, and a 44 nm|12 nm TaN|TaON absorber stack on the mask.

Table 1. Overview of Key Design Requirements

Parameter	Value	Determining Factors
Numerical aperture	0.5 NA	Lithographic modeling.
Wavelength centroid	(13.5 ± 0.05) nm	SEMI standard.
Field size	30 μm x 200 μm	Optical design outcome.
Resolution	~ 8–16 nm	Lithographic modeling.
Chief ray angle on reticle	(6 ± 0.2) degree	SEMI standard.
Image Reduction ratio	5X	Maintained MET3 value.
Bandwidth of transmitted EUV light	> 0.5 nm	Throughput. Weighted over pupil area.
Transmission of EUV light	> 25%	Throughput. Weighted over pupil area.
Track length	474 mm	Maintained MET3 value.
Back working distance	5 mm	Focus sensors. Maintained MET3 value.
M1 mirror clear aperture	92 mm	Design constraints.
M1 aspect ratio (outer diameter : average thickness)	12:1	Design constraints.
M2 mirror clear aperture	250 mm	Design constraints.
Central obscuration (by area)	< 10%	Lithographic modeling.
Apodization uniformity (P-V)/(P+V)	< 6 %	Lithographic modeling.
Aspheric departure	< 60 μm	Design constraints – highest ever reported for EUVL.
Aspheric gradient	< 6 μm/mm	Design constraints.
Wavefront error, field center	< 0.5 nm RMS	Lithographic modeling.
Wavefront error, field edge	< 1.0 nm RMS	Lithographic modeling.
Flare	< 5%	Lithographic modeling.
POB mass	(46 ± 5) kg	Platform requirement.
Operating temperature	(22 ± 0.1) °C	Platform requirement.
Outgassing rate, hydrocarbons	$<10^{-7}$ mBar L/Sec	Contamination budget.

In many cases these requirements came directly from the need to re-use the MET3 platform. The optical track length is an intuitively obvious example as this determines the wafer and mask separation. Likewise, hard limits existed for the mirror diameters and their apex positions. In other cases subtler factors had to be taken into consideration. For example, adjusting the conjugate locations as a third order spherical aberration compensator is limited by stage adjustment ranges. In other cases, design values came about from a compromise on competing effects and the trade-offs were comprehended in a simultaneous system optimization. The goals for high NA, low central obscuration, high working distance, and primary mirror thickness to diameter aspect ratio all pushed against each other. The apex location of the primary (smaller) mirror was a compromise of all of these effects. Similarly, the secondary apex height might have been increased if not for the maximum diameter requirement and the need to leave room for the illumination path at an intended 6° chief ray angle. However, even with these limits, a robust design solution [1] was found which successfully optimizes Petzval curvature and minimizes wavefront error within the requirements.

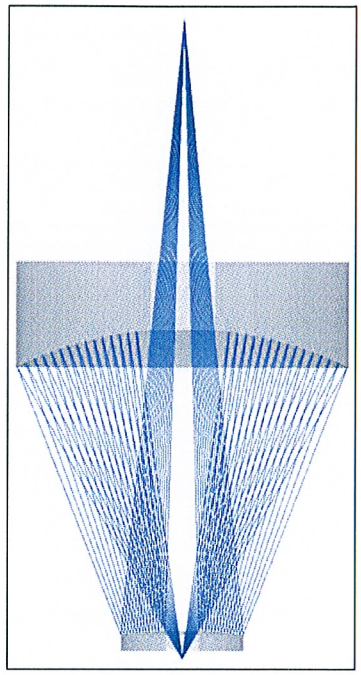

Figure 2. Optical Design of the MET5 POB

3. MIRROR FABRICATION AND METROLOGY

3.1 Past Experience in Fabricating EUV Optics – Zygo

Zygo Corporation has 20 years of experience in fabricating EUV optics and participated successfully as the primary optics supplier in numerous development/production programs for EUV systems. Table 2 provides an overview of these programs.

The improvements of achieved surface accuracy and smoothness over the past 16 years are displayed in Figure 3 in chronological order.

Table 2. Past Programs Developing and Fabrication EUV Optics – Zygo

Customer	Description	Time Period
AT&T	Demonstration Mirror	1993
NTT Japan	3-mirror system	1994
Sandia	3-mirror system	1995
Himeji Institute of Technology	3-mirror system	1997
EUV-LLC	ETS 4-mirror system	1997–1999
EUV-LLC	10X Schwarzchild objective	1998–1999
Large Semi. Company	10X Schwarzchild objective	2002–2003
HIT	30X Schwarzchild objective	2003–2004
Large Semi. CapEx Company	Off-Axis mirror	2002–2005
LLNL	Off-Axis Parabola – FLASH FEL experiment	2007–2008
DESY	Off-Axis Parabola – FLASH FEL experiment	2010
Large Semi. CapEx Company	Off-Axis mirror	2007–Present

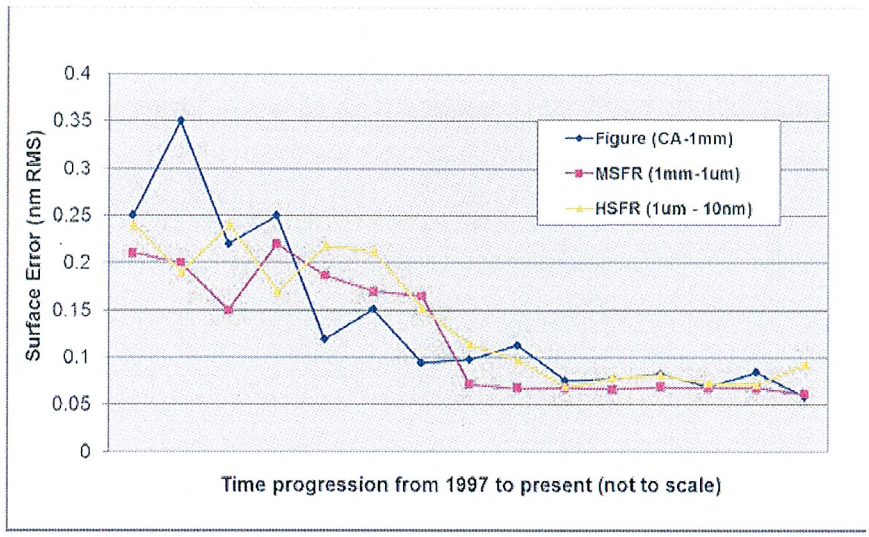

Figure 3. Chronological improvement in achieved full-spectrum mirror surface accuracy and roughness over various ranges of spatial periods: Figure – Clear Aperture (CA) to 1 mm, Mid-Spatial Frequency Range (MSFR) – 1 mm to 1 µm and High-Spatial Frequency Range (HSFR) – 1 µm to 10 nm.

3.2 Power Spectral Density Controlled Optical Fabrication and Metrology

The surface topographies of the MET5 primary and secondary mirrors are best characterized and quantified by using the power spectral density (PSD), which is derived from the Fourier spectra of surface height data. These PSD curves are used to guide the polishing of the optical surfaces. This strategy has been described in earlier literature [7].

Figure 4 displays the achieved PSD on an EUV optic fabricated in the past at Zygo EPO. Note that the PSD has been measured over 6 orders of magnitude of spatial periods. The integrated PSD over any decade of spatial periods measures less than 50 pm RMS. This PSD forms the target performance for the MET5 mirrors.

A technological challenge of the MET5 program is adapting the polishing and metrology techniques used to achieve the results above on aspheres with greater aspheric departure. The larger asphericity (i.e., local change of curvature) represents a challenge for polishing and metrology processes. For a high asphericity, achieving the required smoothness at the higher spatial periods requires careful attention to the design of the polishing processes. For highly aspheric surfaces this process is more complex and requires more individual steps than for spherical surfaces or for surfaces with relatively low aspheric departures. Table 3 compares the maximum nominal aspherical sags and slopes of the MET5 and the MET3 mirrors. These quantities are between a factor of 7 and 12 higher for MET5 than for MET3 mirrors. Note that the maximum aspheric sag of the surface that is represented by its PSD in Figure 4, is slightly less than the sag of the MET3 M1 mirror.

Table 3. Comparison of maximum nominal aspherical sag (departure from a best-fit sphere) and its slope between MET3 and MET5.

Mirror		Max. Aspherical Sag		Max. Aspherical Slope	
	unit >>	µm	λ = 13.5 nm	µm/mm	λ/mm
M1	MET3	4	296	1.2	89
	MET5	46	3407	8.3	615
	MET5/MET3	11.5	11.5	6.9	6.9
M2	MET3	6	444	0.5	37
	MET5	51	3778	3.7	274
	MET5/MET3	8.5	8.5	7.4	7.4

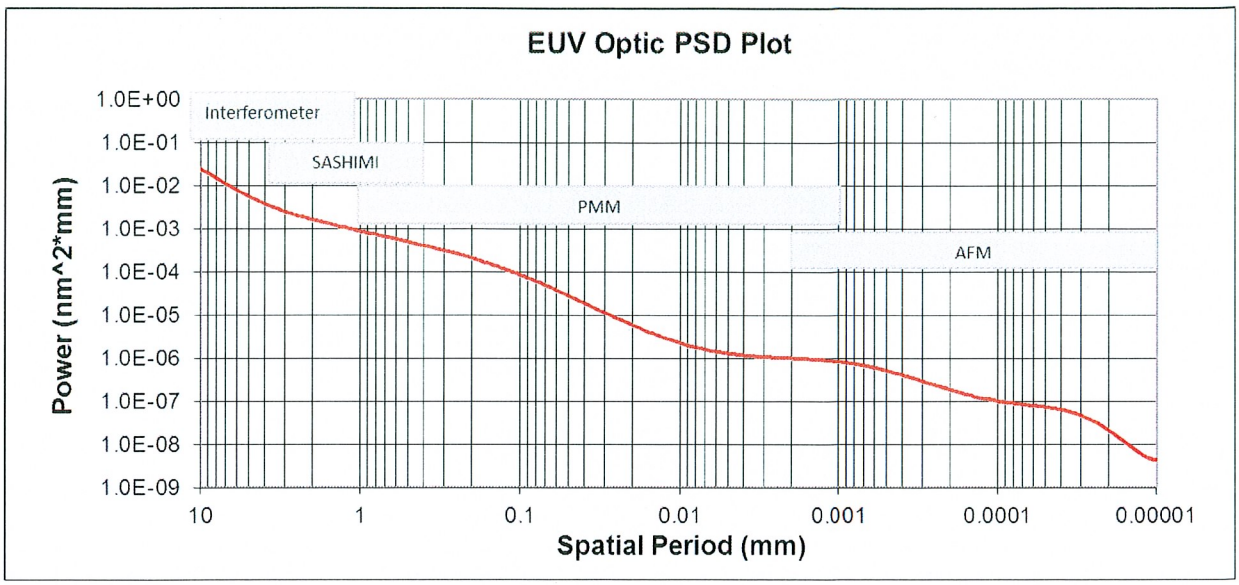

Figure 4. One-dimensional PSD curve with ranges of metrology instruments. These instruments are defined and discussed in Sections 3.5 and 3.6. The overlap of ranges allows for a stitching of individual curves without interpolation.

3.3 Mirror Substrate Fabrication

The MET5 primary and secondary mirrors are complex glass structures. The shaping of the substrates before polishing requires high-precision fabrication and metrology equipment.

The fabrication process begins with a computer-aided design (CAD) solid model of the mirror. The model is imported into computer aided manufacturing (CAM) software where the tool paths for the parts complex geometry are generated and a machining code specific to the targeted computer numerical control (CNC) machine is created. Tool path verification software is employed to ensure the accuracy of the programs.

Figure 5. Five-Axis, Ultrasonic, High-Precision Milling Machines

Zygo EPO employs 5-axis, ultrasonic, high-precision milling machines to create the intricate mirror geometry. Ultrasonic machining marries the traditional rotary grinding action of diamond tools with a pulsing action at rates greater than 10,000X per second. This results in a 3X to 4X higher material removal rate compared to traditional grinding and machined surfaces with very good surface quality and reduced sub-surface damage. An integrated touch probe is used to precisely align the substrate to the machine in order to achieve critical feature placement. The optical surfaces are created using a high-precision aspheric generator. The process uses a series of diamond tools designed to yield a surface with minimal sub-surface damage that is effectively ready to polish. The aspheric generator also uses an integrated touch probe to control the optical thickness and precision fixtures to insure that the asphere is accurately placed on the substrate. Shape compensations that are generated using coordinate measuring machine (CMM) and profilometer data are applied to the tool path in order to achieve an aspheric profile with a very small variation from nominal.

3.4 Optical Surface Polishing

Polishing of the aspheres utilizes computer-controlled optical surfacing (CCOS) technology that has been developed at Zygo EPO. CCOS employs a suite of sub-aperture processes optimized to work on discrete regions of the PSD. CCOS is fundamentally an iterative process. The challenge is to optimize the process selection and the order of process application to predictably improve the targeted PSD region without degrading neighboring regions. For the high aspherical departure MET5 aspheres, polishing tool design and tool material selection are critical for converging on the final specifications, especially towards the higher frequency ends of the mid-spatial frequency range (MSFR) and high-spatial frequency range (HSFR) of the PSD.

Ion beam figuring (IBF) is another critical method of CCOS used on MET5 optics. IBF uses a shaped ion beam and a CNC stage system to figure the surface of the optic and enables sub-nanometer level figuring without significant degradation to the MSFR and HSFR regions of the PSD.

Figure 6. Ion Beam Figuring (IBF) chamber

3.5 Mirror Surface Figure Metrology

Precision CMMs are utilized as feedback in the machining and optical surface generating operations. They have sub-µm accuracy over their respective measurement volumes. Calibration techniques are deployed to achieve accuracies of less than 100 nm. An optical probe is integrated with one of the CMMs for non-contact profilometry.

In the next stage of figuring the aspheres, a profiler, which is capable of providing nanometer level precision over large scan areas, is used to characterize the surface errors. With careful calibration, this profiler measures the profile of the optical surface to better than 20 nm peak-to-valley (P-V).

As the optical surface error is further reduced, a Zygo Verifire Asphere (VFA) interferometer is used to characterize the surface and prepare it for the ultimate optical test, which will measure the optic to the sub-nanometer level. The higher accuracy figure measurements are performed on a dedicated test station designed to meet the demanding requirement of EUV projection optic mirrors. The test uses a computer generated hologram (CGH) as a diffractive null element in a vertical cavity test. A vertical cavity is used in order to respect the as-used gravity orientation of the mirrors. The test cavity is enclosed and all of the motions are remotely controlled to avoid disturbances from the test operator. The test is located in a temperature controlled clean room where pressure and humidity are monitored.

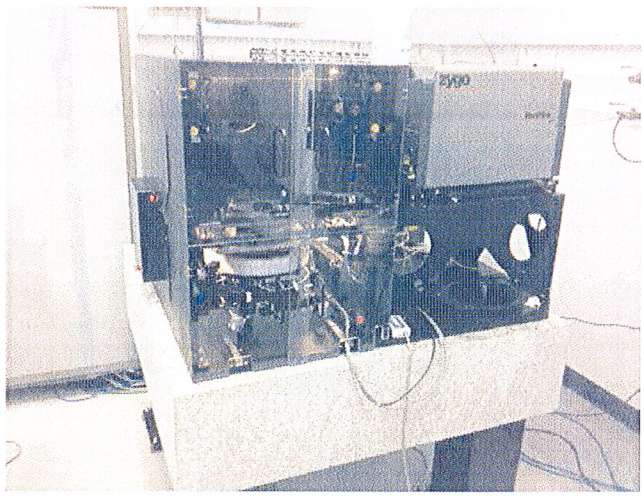

Figure 7. Primary Mirror Optical Test

The actual wavelength of the interferometer is measured with a wave-meter and adjusted for the current environmental conditions. A correction for wavelength-induced error to the test wavefront is applied to the measured part. The diffractive element is designed in-house and fabricated on a substrate polished by Zygo EPO with sub-nanometer transmitted wavefront specification. The diffractive pattern quality is assured by process control and in-process metrology of key parameters allowing subtraction of wavefront error caused by pattern fabrication errors [8]. The MET5 mirrors have special low-stress mounts designed to match the mounts in the integrated POB module. The test mounts and the module mounts are designed to minimize both the amount of stress transmitted to the mirror and the variations between the two sets of mounts. The test calibration consists of several self-compensating absolute tests that are performed *in-situ* in order to quantify and subtract contributions from test optics [9] [10].

The most significant contribution to the uncertainty budget is spherical aberration of low order that can be compensated within some allocation limit. The uncertainty on the non-compensable symmetrical aberration is within the POB transmitted wavefront error budget. The target repeatability for the MET5 component tests is 50 picometer (pm) RMS, a value that was achieved on prior EUV metrology test stations.

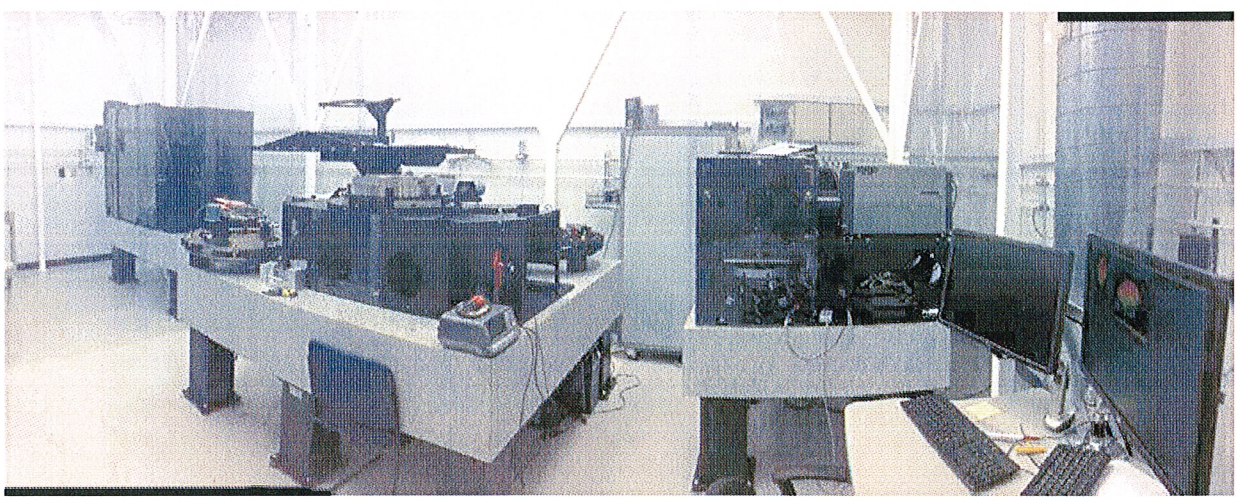

Figure 8. MET5 optical tests (left to right): POB transmitted wavefront test, M2 and M1 mirror surface figure tests.

3.6 Metrology of Mirror Surface Micro-Roughness

Metrology instruments have been selected so that the frequency responses of successive instruments overlap to eliminate any gaps in the PSD (compare Section 3.2).

Enhancing the metrology resolution between full-aperture metrology described in section 3.5 and the phase measuring microscope (PMM) is a Zygo EPO designed and built instrument named Sub-Aperture Surface Height Interferometric Measuring Instrument (SASHIMI). SASHIMI utilizes custom objectives designed to match the curvature of the asphere under test. A white light interferometer and a stage system positions the optic normal to the interferometer and high resolution, sub-aperture images are recorded across the optical surface. To measure the steep slopes of the MET5 aspheres, the field of view (FOV) for the M1 mirror is 10 mm in size and 20 mm for the M2 mirror. To cover the entirety of the optical surface, hundreds of apertures are generated and proprietary software stitches the images together to produce a continuous image of the surface topography. More detail on the SASHIMI method can be found in a publication by Marchetti [11].

The PMM is used to characterize the portion of the mid-spatial frequency range (MSFR) that falls between ~1 mm and 1 μm spatial periods. The instrument has multiple objectives (2.5X and 50X) and an extremely low noise floor of less than 50 pm RMS.

Characterization of the High-Spatial Frequency Range (HSFR) surface errors defined between spatial periods of 1 μm and 10 nm is performed with an atomic force microscope (AFM). The instrument is operated in tapping mode and scans of 10 μm × 10 μm and 1 μm × 1 μm are performed at multiple measurement locations at 512 × 512 resolution. The AFM is crucial for quantifying the surface characteristics in the HSFR. It is crucial to control surface errors in this range well, since they determine the reflectivity of the surface for EUV light.

4. MULTILAYER COATINGS

Both M1 and M2 projection mirrors for the MET5 system are rotationally symmetric aspheres. The angles of incidence (AOI), which are defined from the normal incidence direction in the clear aperture region, shown in Figure 9 for each mirror, range from 4° to 14° for M1 and from 1° to 4° for M2. The height difference between the center and the edge of the reflective surface (sag) is about 3 mm for the M1 mirror and 33 mm for the M2 mirror.

A multilayer coating design was selected where the multilayer period is adjusted in such a way that phase and wavelength of highest reflectivity remain constant at all locations within the mirror clear aperture at the as-designed angles of incidence. The Bragg equation for multilayers dictates that the required period of the multilayer is determined by the incidence angle at each mirror location. The as-designed multilayer thickness variation across the clear aperture of the M1 and M2 mirrors is shown in Figure 9.

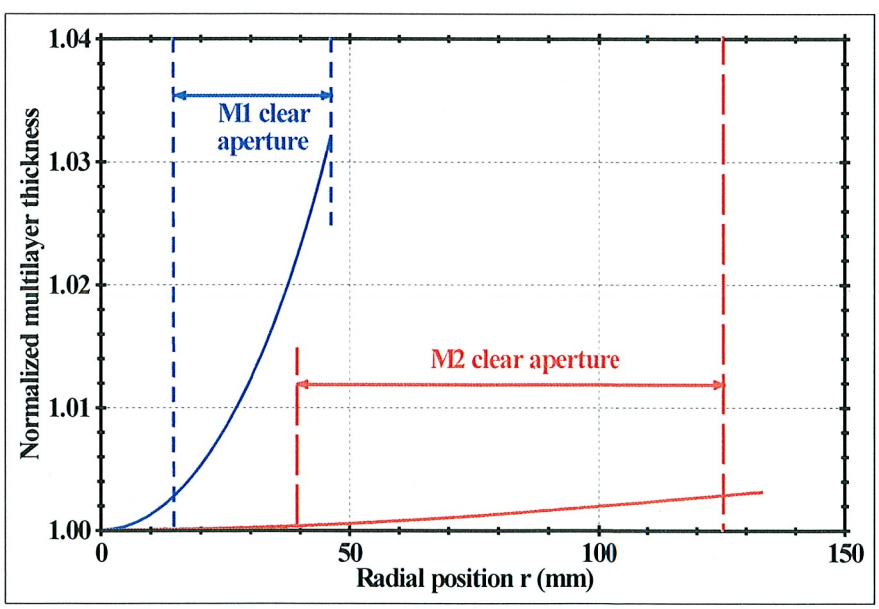

Figure 9. As-designed (ideal) multilayer thickness profiles for the MET5 M1 and M2 mirrors. Clear aperture limits are indicated as vertical dash lines.

The specifications for the MET5 coatings were based on considerations such as throughput, intensity variations (apodization) and system wavefront aberrations. These considerations and their impact on system performance have been discussed in detail in an earlier publication [12]. Based on these metrics, the peak-to-valley multilayer thickness uniformity was set to ±0.2% from the ideal profiles shown in Figure 9.

The non-compensable multilayer-added figure error tolerance was set to 0.08 nm RMS, and the mirror-to-mirror wavelength matching specification was set to (13.5 ± 0.05) nm. Multilayer thin film stress was also required to be minimized, due to the additional figure deformation it induces on the mirrors. The multilayer peak reflectance and FWHM specifications were driven by the overall throughput requirements of the MET5 system and are shown in Table 4 as a function of the number of bilayers (N) in the multilayer. In order to meet all the aforementioned extremely stringent requirements, specially modified Mo/Si multilayer coatings were developed at LLNL for the MET5 POB. The MET5 multilayer coatings were deposited via magnetron sputtering. The Mo/Si coatings demonstrate maximum reflectance, low stress and minimum thickness. The coating thickness was minimized in order to minimize the multilayer-added figure error and was maintained below 250 nm on both M1 and M2 mirrors. Taking into account that the figure deformation induced by coating stress on a mirror is proportional to the product of stress and thickness of the coating, multilayer stress in the range of -100 MPa was achieved on the M1 mirror and -200 MPa on the M2 mirror. More details on this topic will be presented in an upcoming publication. Multilayer thickness profile optimization for the M2 mirror has been completed and is shown in Figure 10. The M2 multilayer coating achieves extremely low peak-to-valley variation and non-compensable added figure error and is well within specifications. Multilayer thickness profile optimization for the MET5 M1 mirror is currently underway and will be discussed in a future publication.

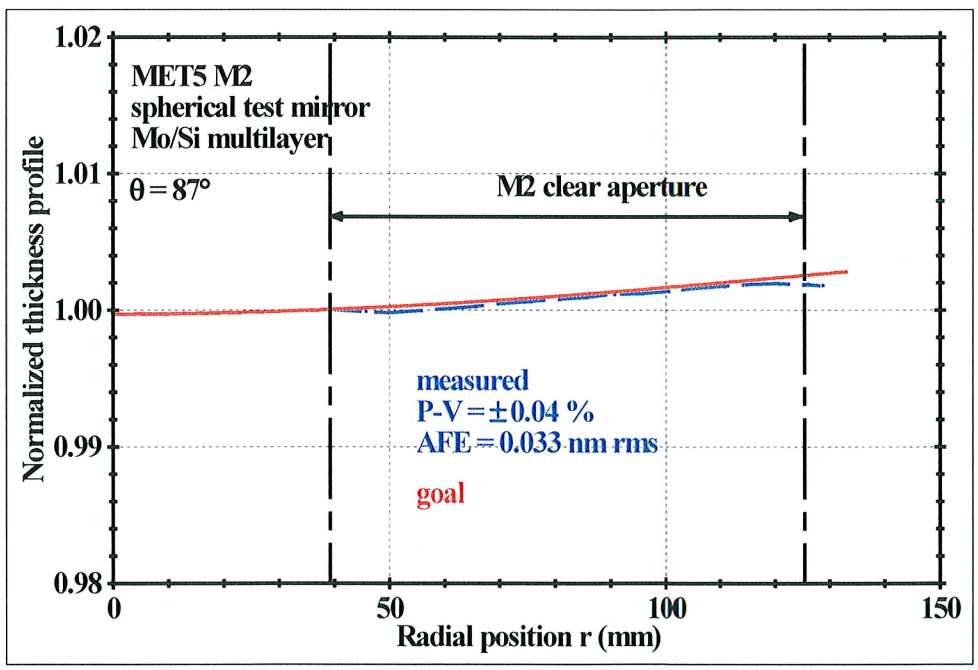

Figure 10. Experimental multilayer thickness profile achieved for the MET5 M2 mirror on a spherical test substrate. The test substrate was the best-fit spherical approximation of the actual M2 aspherical surface. The multilayer coating achieves ±0.04 % peak-to-valley (P-V) thickness variation and 0.033 nm RMS non-compensable added figure error (AFE) and is well within specifications. Measurements were performed at the Advanced Light Source Synchrotron, Lawrence Berkeley National Lab.

Table 4. Peak reflectance and FWHM specifications and goals are shown as a function of number of bilayers for the Mo/Si multilayers in the MET5 system. The peak reflectance values correspond to a substrate with ideal (near-zero) high-spatial frequency roughness.

Number of Bilayers	Peak Reflectance Spec	Peak Reflectance Goal	Bandwidth FWHM Spec	Bandwidth FWHM Goal
20	> 50%	53%	> 0.67 nm	0.77 nm
30	> 58%	63%	> 0.53 nm	0.63 nm
40	> 63%	66%	> 0.48 nm	0.58 nm
50	> 64%	67%	> 0.45 nm	0.55 nm

5. OPTO-MECHANICAL DESIGN AND ASSEMBLY

Once the mirrors have been fabricated and multilayer-coated, they are assembled into the final Projection Optics Box (POB) configuration. The mechanical structure facilitates four critical functions:

- Low-distortion optical mounting
- High-precision optical alignment
- Opto-mechanical (dimensional) stability
- System integration into the MET environment

The structure supporting this Schwarzschild configuration utilizes Super-Invar material with a low Coefficient of Thermal Expansion (CTE). This material is complementary to the mirrors' near-zero CTE substrate material. Each mirror attaches to mounting rings via low-distorting bipod structures containing integrated flexures. The larger concave secondary mirror is mounted to the main mount ring which also provides kinematic mounting to the MET system. The smaller convex primary mirror is mounted to a slaved mount ring controlled by the main mount ring through a set of actuator-driven hexapods structures. This hexapod assembly allows precise alignment to focus and image at the wafer plane below the small primary mirror. This design concept has been derived from the incumbent MET3 design [13].

Figure 11. Opto-mechanical design of the POB (mirrors displayed in light blue; some features omitted for clarity)

As discussed earlier, the dimensional envelope of the MET5 POB must conform to the legacy MET3 POB while increasing performance almost three-fold associated with the newer 0.5 NA design. The actuator-driven hexapods drive the M1 stage motion with a four-fold improvement in the z-axis precision, a twice-fold improvement in the lateral precision, and a four-fold improvement in the tilt precision compared to the MET3 system.

The high-performance optical geometry of the MET5 necessitates that the M1 mirror have a 2.2X higher cross-sectional aspect ratio (compare Table 5) than the corresponding MET3 mirror. The aspect ratio is defined as the ratio of the mirror's outer diameter to its average thickness.

Applying the "rule of thumb" that the stiffness of an object is proportional to its aspect ratio squared, the stiffness of the MET5 M1 is about five times weaker and will hence be five times more sensitive to mounting- and coating-induced stresses than the MET3 M1 (compare Table 5). To mitigate this effect, an innovative mechanical isolation system with a 5X reduction in mount-induced stress and advanced assembly procedures are implemented to achieve the required isolation. The multilayer coatings were also optimized for lowest stress, as is discussed in Section 4.

Table 5. Aspect Ratios and their squares of M1 mirrors – comparison MET3 and MET5.

M1 Mirror	Aspect Ratio	Aspect Ratio ^2
MET3	5.4	29
MET5	11.7	137
MET5/MET3	2.2	4.7

The design of the opto-mechanical structure was supported by a structural and dynamic finite element analysis (FEA).

Ensuring that all the mirror support mounts and attachment structures are precisely mated without residual forces or moments and stable under acceleration loads during handling and shipping is a significant challenge. The MET5 assembly process improves upon the original MET3 assembly performed at LLNL by integrating new mechanical design aspects, new assembly tooling designs, and contact/non-contact metrology to drastically minimize the mirror mounting stresses. Assembly is performed in our consolidated EUV cleanroom facility combining the POB assembly and the coordinate measuring machine (CMM) functions in a single environmentally-controlled room without contamination risk. Additionally, contamination control has been a requirement for the design and material selection of POB components, fixtures and tooling.

Lastly, comprehensive acceptance testing includes outgassing verification and stability under thermal, shock and vibrational loads.

6. METROLOGY OF THE TRANSMITTED WAVE FRONT

The POB optical test is used to align and qualify the wavefront of the projection optic system to 0.5 nm RMS at the center of the field and 1.0 nm RMS at the edge of the field. The test is designed to operate at 633 nm and uses a Zygo MST wavelength-shifting interferometer with specially designed optics.

All of the test optics are fabricated in-house to sub-nanometer specifications and absolute self-referencing metrology techniques have been used to qualify these optics [9] [10]. As shown in Figure 12, the interferometer illuminates the MET5 system from the reticle side with an 0.1-NA beam. The wavefront transmitted through the system is retro-reflected by a high precision 0.5-NA retro-sphere back to the interferometer. The double pass test configuration gives a greater sensitivity to error and misalignment of the POB compared to a single pass system. Due to the high NA of the beam, a displacement of 13 nm of the image (wafer) plane causes 0.5 nm RMS of defocus wavefront error, as much as the entire wavefront error specification. This sensitivity is 2.8x higher than for a 0.3 NA lens[§]. Although the focus error can be easily adjusted, the other axial distances between the POB components remain quite sensitive. The entire system test is mounted on a rotation stage that facilitates the alignment, calibration and qualification of the system. The POB has to be measured at the center and at off-axis points in order to determine what adjustments are needed to obtain the optimum wavefront. To help with the measurement, the test optics are mounted on translation stages that can be remote controlled with high-precision position sensor feedback to the different field points. The result of the measurement is analyzed to deconvolve aberrations into

---

[§] The defocus wavefront error scales with NA^2.

adjustments of the M1 mirror, image and object conjugate positions and best fit location of the optical axis. The required M1 mirror adjustments are then turned into commands to the hexapod control system to change the length of the hexapod legs appropriately.

The wavefront specification of 0.5 nm RMS corresponds to $1/30^{th}$ of a wave at 13.5 nm or $1/1300^{th}$ of a wave at 633 nm. Although it appears like a significant challenge to measure to better than $1/1000^{th}$ of a wave, modern phase-shifting interferometry using a stable and proven light source is capable of supporting the required measurement precision. The obvious drawback of measuring the fully coated MET5 POB in the visible is the phase-shift associated with the EUV multilayer. The phase-shift associated with the multilayer used in the visible and at 13.5 nm must be fully understood in order to interpret the visible measurement correctly.

Although some processes applied in the fabrication of the MET5 POB have risks and uncertainties, a high level of engineering went into qualifying and understanding these risk and uncertainties. In the unlikely case our processes have unqualified biases, the ultimate test of performance is the measurement of the wavefront in the POB test.

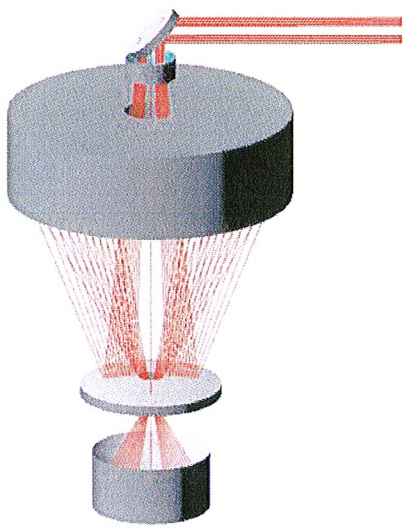

Figure 12. POB Optical Test Layout

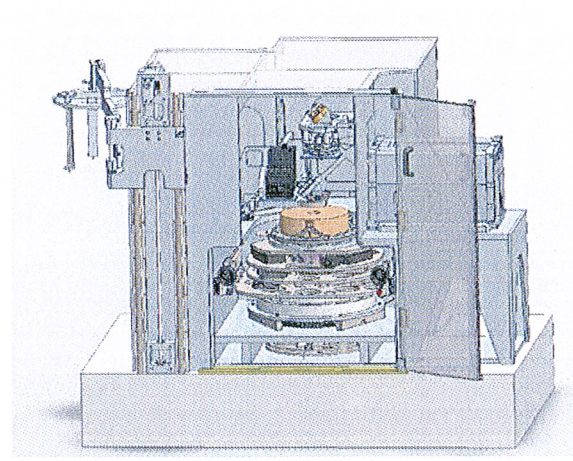

Figure 13. Mechanical Model of the POB Optical Test

7. LITHOGRAPHIC MODELING

As mentioned in the introduction, the primary purpose of the MET5 system is to provide very early learning into the extendibility of EUV lithography to 12 nm half-pitch and below. Rigorous aerial image modeling has been performed to study the capabilities of the MET5 optical system in this regime. In this section we present some representative results. The modeling results in Figure 14 rely on rigorous 3D modeling including a mask with a full multilayer stack. The absorber structure is 70 nm TaN. We further assume the field center design.

We begin by analyzing the performance printing 12 nm lines and spaces using a general-purpose unpolarized annular illumination with an inner sigma of 0.36 and an outer sigma of 0.93. This illumination condition will be readily available on both the Albany and Berkeley systems except that the light is polarized on the Berkeley system. We consider the case of un-shadowed lines. The left side of Figure 14 shows the resulting Bossung plot and exposure latitude versus depth of focus (DOF) plot. Each line in the Bossung plot represents a 6% dose change. The DOF predictions are based on an acceptable CD variation of ±10%.

Next we consider the case of 8-nm lines and spaces with extreme dipole illumination. We further consider the lines to be in the shadowed direction with an angle of incidence of 6 degrees (lines running in the x direction) and we assume linearly polarized light in the x direction. The pole offset is 0.85 and the pole radius is 0.15. This configuration will be available on

the Berkeley system. We again find a depth of focus greater than 100 nm. The right side of Figure 14 shows the resulting Bossung plot and exposure latitude versus depth of focus plot.

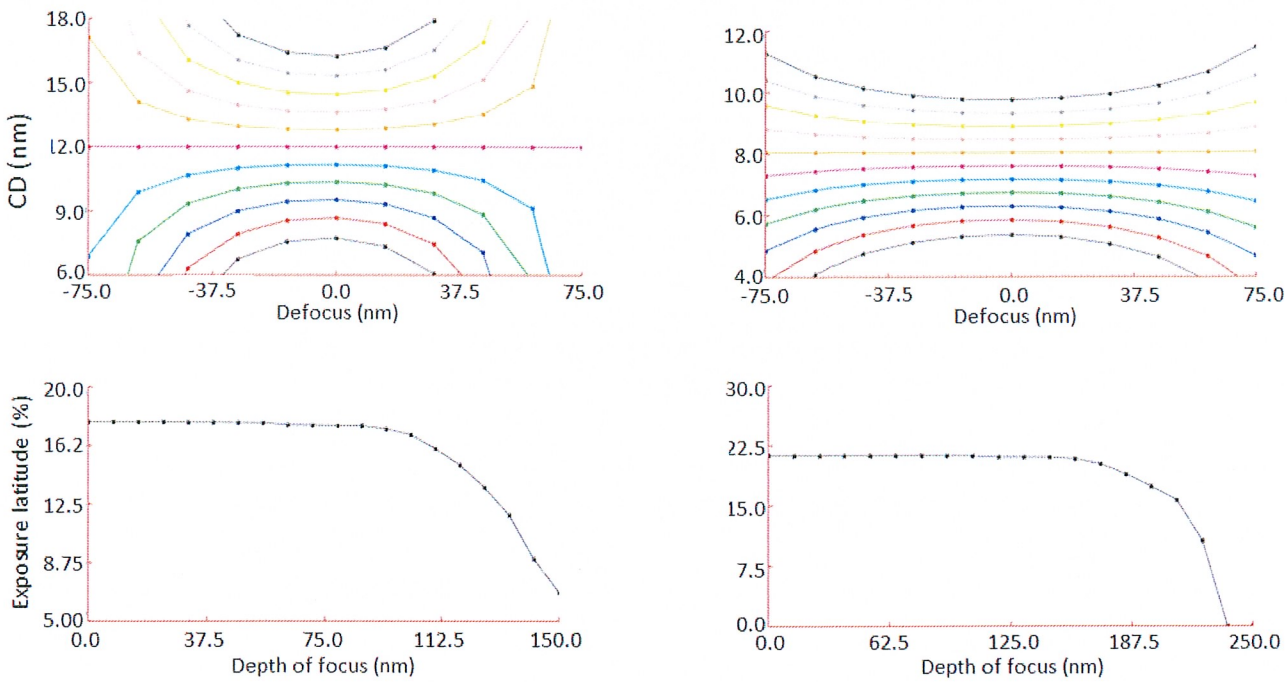

Figure 14. Bossung curve (top) and Exposure latitude versus DOF (bottom) for 12 nm line space printing under annular illumination (left side) and for 8 nm line space printing under dipole illumination (right side). Each line in the Bossung plots represents a 6% dose change. The DOF plots are based on ±10% CD change.

8. SUMMARY

The need for improved lithographic performance of the MET5 Project Optics Module, while maintaining the dimensional envelope of the incumbent MET3 module, resulted in numerous technological and programmatic challenges. These challenges have been thoroughly analyzed and solutions have been identified.

- Under the lead of Zygo Corporation, a multi-disciplinary team with experience in EUVL optics has been formed and an extensive development program is under way.
- The optical and opto-mechanical design of the module has been completed.
- All needed equipment, tooling and test optics has been designed, fabricated and assembled.
- The processes to shape, polish and coat the mirrors are currently being developed on pathfinder mirrors. Furthermore, the process to assemble and align the module is under test with a pathfinder module.

9. ACKNOWLEDGEMENTS

Beyond the authors of this publication a wider group of contributors has been and/or continues to be critical to the success of building the two SEMATECH 0.5 NA projection optics. The authors recognize their significant contribution. We are grateful to the following individuals: Dan Bajuk, Grace Brauer, Matt Bjork, Charlie Chen, Mark Cordier, John Davison, Melissa Evans, Richard Fisher, Klaus Freischlad, Adam Goyner, Dennis Hancock, Sam Hardy, Ali Korehi, Vishal Lamba, Stephen Mielke, Ann Morton, Bill Ojala, Aurelie Overbay, Daniel Pierce, Jack Pinkham, Bill Reichman, Lian Shao, Glen Smith, Nick Swan, Jay Thomas, Bruce Truax, Marc Tricard, Jim Verrico, Bob Watts, Jeremy Watts, Richard Wieczorek at Zygo; Jeff Robinson, Mónica Fernández-Perea, Jay Ayers, Shannon Ayers, Sherry Baker and Aaron Sperry at LLNL; Senajith Rekawa,

Geoff Gaines and Mark West at LBNL; Arash Gorbani at Hyperion Development; and Bryan Rice and Stefan Wurm at SEMATECH.

In addition we would like to express our appreciation to the support staff at all facilities. The coating development was performed under the auspices of the U.S. Department of Energy by Lawrence Livermore National Laboratory under Contract DE-AC52-07NA27344. EUV metrology work to support the coating development was performed under the auspices of the U.S. Department of Energy at Lawrence Berkeley National Laboratory under Contract DE-AC02-05CH11231.

10. REFERENCES

[1] M. Goldstein, R. Hudyma, P. Naulleau and S. Wurm, "Extreme-ultraviolet microexposure tool at 0.5 NA for sub-16 nm lithography," *Opt. Lett.* **33**(24), 2995 – 2997 (2008)

[2] M Booth et al.,"High-resolution EUV imaging tools for resist exposure and aerial image monitoring" " *Proc. SPIE, Vol. 5751, Emerging Lithographic Technologies IX*, 78 (2005)

[3] Patrick Naulleau et al., "Recent results from the Berkeley 0.3-NA EUV microfield exposure tool" , *Proc. SPIE*, Vol. 6517, 65170V (2007)

[4] Moore, Gordon E. (1965). "Cramming more components onto integrated circuits" (PDF). *Electronics Magazine*. p. 4. Retrieved 2006-11-11.

[5] J. S. Taylor, D. Sweeney, R. Hudyma, L. Hale, T. Decker, G. Kubiak, W. Sweatt, and N. Wester "EUV Micro-exposure tool (MET) for near-term development using a high NA projection system," *2nd International Workshop on EUV Lithography*, Burlingame CA (2000.)

[6] A. Brunton, J. Cashmore, P. Elbourn, G. Elliner, M. Gower, P. Grunewald, M. Harman, S. Hough, N. McEntee, S. Mundair, D. Rees, P. Richards, V. Truffert, I. Wallhead, M. Whitfield, "High-resolution EUV microstepper tool for resist testing and technology evaluation," *Proc. SPIE* 5448, 681 (2004).

[7] U. Dinger, et. al., "Mirror substrates for EUV-lithography: progress in metrology and optical fabrication technology", *Proc. SPIE* Vol. 4146, 35-46 (2000)

[8] S. M. Arnold and R.N. Kestner, "Verification and certification of CGH aspheric nulls", *Proc. SPIE* 2536, Optical Manufacturing and Testing, 117 (September 8, 1995)

[9] C. J. Evans and R. N. Kestner, "Test optics error removal" *Appl. Opt.* ,Vol. 35, 1015–1021 ,1996.

[10] Klaus R. Freischlad, "Absolute Interferometric Testing Based on Reconstruction of Rotational Shear", *Appl. Opt.*, Vol. 40, Issue 10, pp. 1637-1648 (2001)

[11] Louis A. Marchetti, "Fabrication and Metrology of 10X Schwarzschild optics for EUV imaging", *Proc. SPIE* 5193, (2004)

[12] R. Soufli, R. M. Hudyma, E. Spiller, E. M. Gullikson, M. A. Schmidt, J. C. Robinson, S. L. Baker, C. C. Walton, and J. S. Taylor "Sub-diffraction-limited multilayer coatings for the 0.3 numerical aperture micro-exposure tool for extreme ultraviolet lithography", *Appl. Opt.* **46**, 3736-3746 (2007).

[13] L.C. Hale, et.al., "High-NA Camera for an EUVL Microstepper", US Dept of Energy, Lawrence Livermore National Laboratory, UCRL-JC-140201 (2000)

[14] P. Naulleau, K. Goldberg, E. Anderson, K. Bradley, R. Delano, P. Denham, B. Gunion, B. Harteneck, B. Hoef, H. Huang, K. Jackson, G. Jones, D. Kemp, A. Liddle, R. Oort, A. Rawlins, S. Rekawa, F. Salmassi, R. Tackaberry, C. Chung, L. Hale, D. Phillion, G. Sommargren, J. Taylor, "Status of EUV microexposure capabilities at the ALS using the 0.3-NA MET optic," Proc. SPIE 5374, 881-891 (2004).

[15] Chris Anderson, Dominic Ashworth, Lorie Mae Baclea-An, Suchit Bhattari, Rikos Chao, Rene Claus, Paul Denham, Ken Goldberg, Andrew Grenville, Gideon Jones, Ryan Miyakawa, Ken Murayama, Hiroki Nakagawa, Senajith Rekawa, Jason Stowers, Patrick Naulleau, "The SEMATECH Berkeley MET: demonstration of 15-nm half-pitch in chemically amplified EUV resist and sensitivity of EUV resists at 6.x-nm," Proc. SPIE 8322 (2012).

[16] Jeff Meute, Georgia Rich, Stefan Hien, Kim Dean, Carolyn Gondran, Julian Cashmore, Dominic Ashworth, Jim Webb, Lisa Rich, Paul Dewa, "Contamination and Degradation of 157nm Stepper Optical Components - Field Experience at International SEMATECH", Proc. SPIE 4691 (2002)

[17] Emil C. Piscani, Shane Palmer, Chris Van Peski, "Demonstration of sub-45nm features using azimuthal polarization on a 1.30NA immersion microstepper", Proc. SPIE 6520 (2007)

[18] Klaus Lowack, Andy Rudack, Kim Dean, Matt Malloy Mike Lercel, "The EUV Resist Test Center at SEMATECH-North", Proc. SPIE 6151 (2006)

DISCLAIMER

This document was prepared as an account of work sponsored by the United States Government. While this document is believed to contain correct information, neither the United States Government nor any agency thereof, nor The Regents of the University of California, nor any of their employees, makes any warranty, express or implied, or assumes any legal responsibility for the accuracy, completeness, or usefulness of any information, apparatus, product, or process disclosed, or represents that its use would not infringe privately owned rights. Reference herein to any specific commercial product, process, or service by its trade name, trademark, manufacturer, or otherwise, does not necessarily constitute or imply its endorsement, recommendation, or favoring by the United States Government or any agency thereof, or The Regents of the University of California. The views and opinions of authors expressed herein do not necessarily state or reflect those of the United States Government or any agency thereof or The Regents of the University of California.

This work was supported by the Director, Office of Science, of the U.S. Department of Energy under Contract No. DE-AC02-05CH11231.